

Thermal Behavior Variations in Coating Thickness Using Pulse Phase Thermography

Shrestha Ranjit*, Yoonjae Chung* and Wontae Kim**†

Abstract This paper presents a study on the use of pulsed phase thermography in the measurement of thermal barrier coating thickness with a numerical simulation. A multilayer heat transfer model was used to analyze the surface temperature response acquired from one-sided pulsed thermal imaging. The test sample comprised four layers: the metal substrate, bond coat, thermally grown oxide and the top coat. The finite element software, ANSYS, was used to model and predict the temperature distribution in the test sample under an imposed heat flux on the exterior of the TBC. The phase image was computed with the use of the software MATLAB and Thermofit Pro using a Fourier transform. The relationship between the coating thickness and the corresponding phase angle was then established with the coating thickness being expressed as a function of the phase angle. The method is successfully applied to measure the coating thickness that varied from 0.25 mm to 1.5 mm.

Keywords: Non-Destructive Testing (NDT), Thermal Barrier Coatings (TBC), Pulse Phase Thermography, Thickness Measurement

1. Introduction

Coating refers to the layers applied to the surface of an object, usually known as substrate. The primary purpose of coatings are decoration and protection of the substrate [1]. Several types of coatings such as thermal barrier coatings (TBCs), microwave absorption coatings, anti-corrosion coatings, biochemical protection coatings and functional coatings have been widely used in modern industries to prolong the life of components from oxidation and corrosion, potential hazards and erosion by particulate debris [2]. TBCs are applied to combustion chamber walls, blades, vanes and exhaust nozzles in gas turbines [3-5]. TBC coating insulates the substrate from the heat of the gas path and is increasing its importance for performance benefits. Every 0.025 mm of TBC thickness provides up to 17 to 33°C temperature reduction depending on the TBC ceramic structure and the level of convective

cooling [6].

The coating thickness is not only the parameter of the geometrical property of the coating, but also an important indicator for evaluating the coating quality performance and service life. Thus the effective non-destructive testing for the measurement of coating thickness is of great significance. There is a variety of methods such as magnetic gauges, eddy current, ultrasound, ray, terahertz etc. to inspect the thickness of the coatings. However, they all have certain limitation such as eddy current suffers from manual scanning and ultrasonic suffers from size and shape of the target object [7-9].

Infrared thermography (IRT) is an emerging nondestructive testing and evaluation (NTD&E) technique with many advantages such as non-contact, high speed and large area of observation. IRT is a thermal radiation measurement technique to detect spatial variations in the measured surface temperature pattern. To a greater

[Received: July 13, 2016, Revised: August 15, 2016, Accepted: August 16, 2016] *Department of Mechanical Engineering, Graduate School, Kongju National University, Cheonan 31080, Republic of Korea, **Division of Mechanical & Automotive Engineering, Kongju National University, Cheonan 31080, Republic of Korea, †Corresponding Author: kwat@kongju.ac.kr
© 2016, Korean Society for Nondestructive Testing

extent, IRT has been used in the inspection of thermos-physical properties, sub-surface defects and features, coating thickness and hidden corrosion, etc. IRT involves two classes, passive thermography and active thermography. With respect to the heating procedure, active thermography could be further subdivided into various classes such as pulsed thermography, lock-in thermography, pulsed phase thermography, step heating, vibro-thermography. In the active approach of NDT&E, pulsed thermography (PT) and lock-in thermography (LIT) are the most commonly used approaches [10-16].

This paper focuses on the development of measurement technique to measure the coating thickness. The pulsed phase thermography (PPT) is taken into consideration to acquire the physical insight of thermal phenomena occurring during and after thermal excitation of TBCs structures. A finite element model (FEM) has been used to examine the thermal behaviour of the variations in the TBCs layer. Fourier transform was used to extract the phase angle of pulsed thermographic data. Then the relationship between the coating thickness and its corresponding phase angle was determined and expressed as a function of phase angle.

2. Materials and Methods

2.1. Pulse Phase Thermography

PPT is an active thermographic method. As shown in Fig. 1, the PPT is carried out in reflection mode, where the heat source and IR camera are positioned facing the same surface of the component. When a pulsed thermal energy is excited on the front surface of the test sample, some part of the sample on the surface is heated instantaneously to a high temperature. Then the heat transfer took place from the heated surface to the interior part of the sample, resulting in a continuous decrease of surface

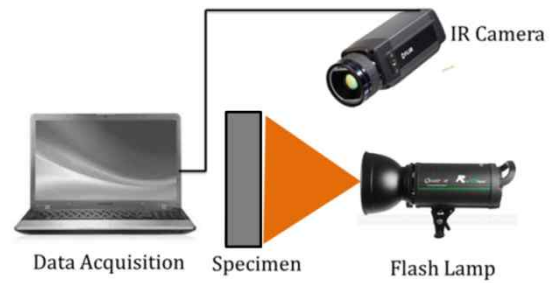


Fig. 1 Schematic of experimental setup for PT system

temperature at consecutive time instants. And the surface temperature data are processed in the phase angle data by using Fourier transform. Hence, PPT combines the heat application and data processing techniques from two established thermography methods; the experimental procedure of PT and the result analysis of LIT. Moreover, it combines the advantages of PT and LIT and also reduces their disadvantages at the same time [17-19].

The temperature rise caused by pulse heating of the surface of a semi-infinite sample can be expressed as Eq. (1) [20],

$$T = \frac{Q}{2\sqrt{\pi k \rho C t}} \quad (1)$$

where T [$^{\circ}\text{C}$] is the temperature rise at time t after the flash heating, Q [$\text{W}/\text{m}^2\rho$] is the energy deposited on the surface, k [$\text{W}/\text{m}^{\circ}\text{C}$] is the thermal conductivity, $[\text{kg}/\text{m}^3]$ is the density of the material and C [$\text{J}/\text{kg}^{\circ}\text{C}$] is the specific heat capacity of the sample material.

The Fourier transform can be used to extract phase angle information from pulsed thermographic data. The Fourier transform can be expressed as Eq. (2) [21,22],

$$F_n = \Delta t \sum_{k=0}^{N-1} T(k\Delta t) \exp \frac{j2\pi nk}{N} = Re_n + Im_n \quad (2)$$

In this case, real and imaginary parts of the complex transform are used to estimate the phase angle and expressed as Eq. (3),

$$\phi_n = \tan^{-1} \left(\frac{Im_n}{Re_n} \right) \quad (3)$$

2.2. Sample

To simulate the PPT inspection, 3-D heat flow finite element model has been considered by using a finite element modelling software 'ANSYS Version 15.0'. TBC with 4 layers, namely, ceramic top coat, thermally grown oxide (TGO), metallic bond coat, and super alloy substrate were considered. Fig. 2 and Fig. 3 shows the geometrical details and the finite element model of test specimen respectively. During meshing, physical preference was considered as mechanical with relevance 100, the relative centre was kept in fine mode and proximity and curvature was kept on in advanced size function. A tetrahedral meshing was adapted as a way to calculate temperature variations with sufficient spatial resolution. The resulting mesh had 78,071 elements and 159,785 nodes. The Table 1 shows the thermo-mechanical properties of TBCs layer considered in the analysis.

During simulation, it is assumed that the specimen surface is submitted to a short heating pulse utilizing a high power optical source of 9 KJ and the duration of the pulse is 10 milliseconds.

3. Results and Discussions

The response to the applied heat flux with the reflection method was simulated using the transient analysis over a period of 6 seconds. Fig. 4 shows the thermal images acquired at 0.06 s, 1 s, 2 s, 3 s, 4 s and 5 s. It can be observed that the thick coating attains a maximum temperature when compared to the thin coatings. The Fig. 5 shows the surface temperature decay of coating with different thickness with respect to time. Due to the very

Table 1 Thermos-mechanical properties of TBCs layers

Layers	Density (Kg/m ³)	Conductivity (W/mk)	Heat capacity (J/kg.K)
TC	3610	0.9	505
BC	3984	3.3	755
TGO	7380	10.8	501
Substrate	4620	21.9	522

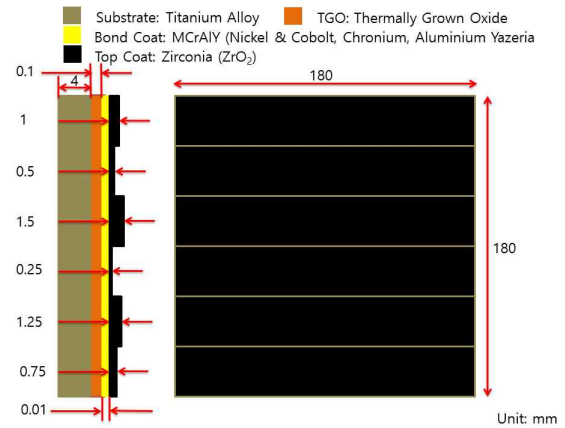


Fig. 2 Geometrical details of the test sample

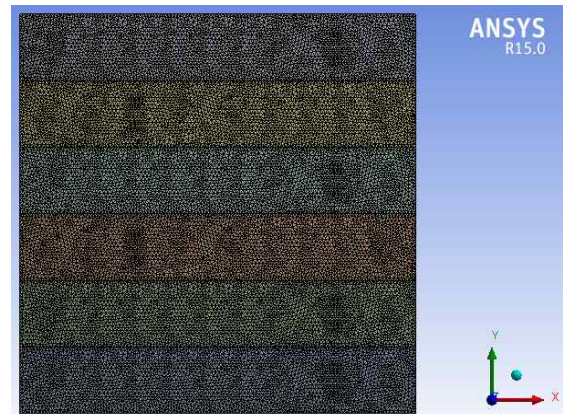


Fig. 3 FEA model with meshing

short heat impulse time the temperature rise is faster than its decay. As the time passes, due to thermal diffusion in all directions, the temperature on the sample surface trends towards the equilibrium again. As determined within the Fig. 5, it is observed that the cooling process of the specimen is almost over in 5 seconds. The pulsed thermographic images were then post-processed to determine the phase angle. The Fourier transform was performed in post

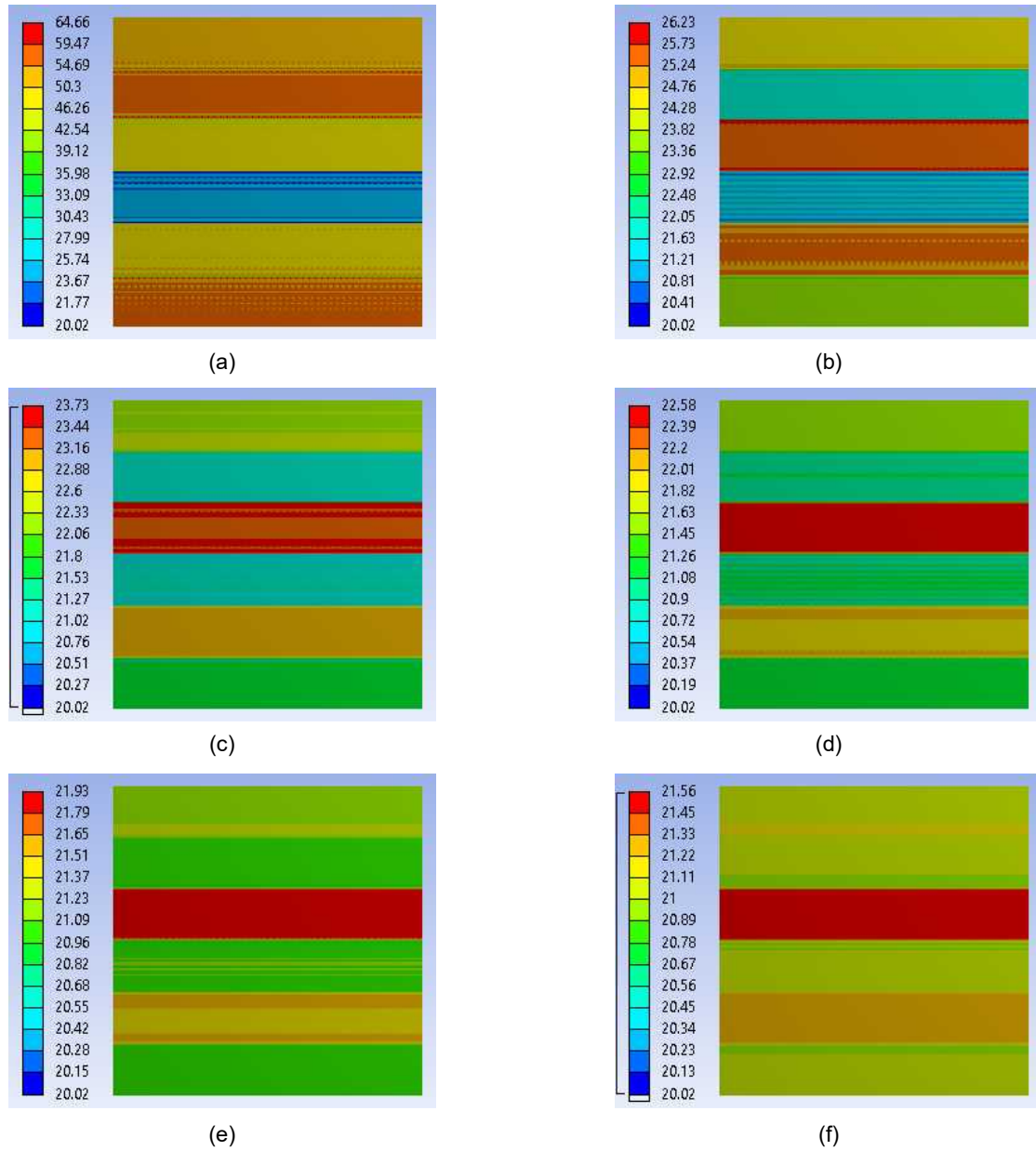


Fig. 4 Pulsed thermographic images at different time interval, (a) time 0.06 s, (b) time 1 s, (c) time 2 s, (d) time 3 s, (e) time 4 s, (f) time 5 s

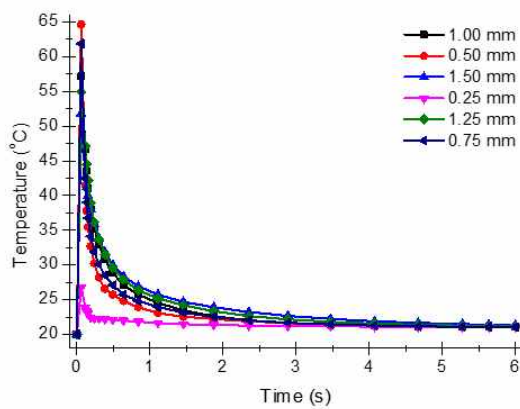


Fig. 5 Surface temperature decay profile



Fig. 6 Phase image acquired with the Fourier transform

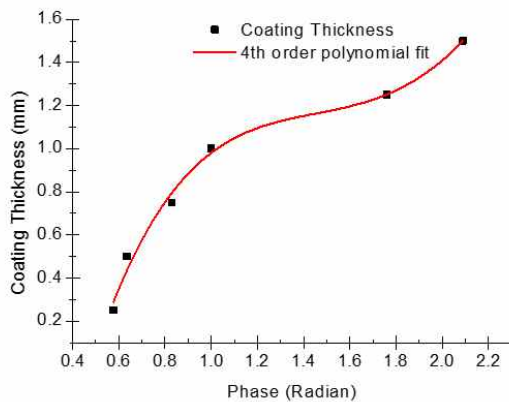


Fig. 7 Coating thickness calibration curve

Table 2 Predicted coating thickness and error percentage

Actual thickness (mm)	Calculated Phase angle (radian)	Predicted thickness (mm)	Error (%)
0.25	0.577	0.289	15.69
0.5	0.635	0.435	12.91
0.75	0.829	0.794	5.90
1	1	0.980	1.98
1.25	1.760	1.251	0.12
1.5	2.090	1.5	0.02

processing of pulsed thermographic images with the MATLAB programming language and ThermoFit Pro software. The Fig. 6 shows the computed phase image. The Fig. 7 shows the relationship between the coating thickness and the corresponding phase angle. With the 4th order polynomial fitting, the coating thickness can be expressed as a function of phase as expressed in Eq. (4),

$$T = -0.17\theta^4 + 1.88\theta^3 - 6.02\theta^2 + 7.90\theta - 2.6 \quad (4)$$

Comparing the predicted coating thickness with the actual coating thickness, the accuracy of the coating thickness measurement is shown in Table 2. From the table, it is observed that the error percentage involved in measurement is within the acceptable limit though error present in thin coatings is high as compared to thick

coatings. It is due to the reason that the mesh size is not enough for the thin coatings. It is expected that the error percentage could be reduced by changing the mesh size and enhancing the mesh quality of thin coatings.

4. Conclusions

In this work, coating thickness measurement method was developed by using pulse phase thermography. A finite element modelling scheme using 'ANSYS Version 15' is proposed to completely simulate the pulse phase thermography. Variation in the temperature of IR thermograms and its corresponding phase angle is the key to measure the thickness of the coating. The method is successfully applied to measure the thickness of coating varied from 0.25 mm to 1.5 mm.

Acknowledgement

This work was supported by the National Research Foundation of Korea (NRF) grant funded by the Ministry of Education, Science and Technology (NRF-2014R1A1A2054595) and the Human Resources Development Program (No. 20154030200940) of the Korea Institute of Energy Technology Evaluation and Planning (KETEP) grant funded by the Korea government Ministry of Trade, Industry and Energy.

References

- [1] A. Mathiazhagan and R. Joseph, "Nanotechnology - A new prospective in organic coating-review," *International Journal of Chemical Engineering and Applications*, Vol. 2, No. 4, p. 225 (2011)
- [2] R. V. Hillery, N. Bartleti, H. Bernstein, R. Davis, H. Herman, L. Hsu, J. Murphy, R. Rapp, J. Smith and J. Stringer, "Coatings for high-temperature structural materials:

- trends and opportunities," *National Materials Advisory Board Report, National Academy Press, Washington, DC* (1996)
- [3] F. Cernuschi, "Can TBC porosity be estimated by non-destructive infrared techniques? A theoretical and experimental analysis," *Surface and Coatings Technology*, Vol. 272, pp. 387-394 (2015)
- [4] S. Akwaboa, P. Mensah, E. Beyazouglu and R. Diwan, "Thermal modeling and analysis of a thermal barrier coating structure using non-Fourier heat conduction," *Journal of Heat Transfer*, Vol. 134, No. 11, pp. 111301 (2012)
- [5] L. Wang, D. Li, J. Yang, F. Shao, X. Zhong, H. Zhao, K. Yang, S. Tao and Y. Wang, "Modeling of thermal properties and failure of thermal barrier coatings with the use of finite element methods: A review," *Journal of the European Ceramic Society*, Vol. 36, No. 6, pp. 1313-1331 (2016)
- [6] D. M. Nissley, "Thermal barrier coating life modeling in aircraft gas turbine engines," *Journal of Thermal Spray Technology*, Vol. 6, No. 1, pp. 91-98 (1997)
- [7] J. Zhang, X. Meng and Y. Ma, "A new measurement method of coatings thickness based on lock-in thermography," *Infrared Physics & Technology*, Vol. 76, pp. 655-660 (2016)
- [8] S. Mezghani, E. Perrin, J. Bodnar, J. Marthe, B. Cauwe, and V. Vrabie, "Evaluation of heterogeneity of paint coating on metal substrate using laser infrared thermography and eddy current," *Evaluation*, Vol. 1, pp. 20665 (2015)
- [9] M. M. Kumar, K. Vikrant, M. Swamy, M. Rawat and R. Markandeya, "Theoretical estimation of thickness variation in thermal barrier coatings by using pulse phase thermography," *11th International Conference on Quantitative Infrared Thermography*, Naples, Italy (2012)
- [10] S. Ranjit and W. T. Kim, "Detection of subsurface defects in metal materials using infrared thermography; image processing and finite element modeling," *Journal of the Korean Society for Nondestructive Testing*, Vol. 34, No. 2, pp. 128-134 (2014)
- [11] S. Ranjit and W. Kim, "Detection and quantification of defects in composite material by using thermal wave method," *Journal of the Korean Society for Nondestructive Testing*, Vol. 35, No. 6, pp. 398-406 (2015)
- [12] S. Ranjit and W. Kim, "Research on defects detection by image processing of thermographic images," *International Journal of Engineering and Technology*, Vol. 7, No.5, pp. 1849-1855 (2015)
- [13] S. Ranjit, W. Kim, and J. Park, "Numerical simulation for quantitative characterization of defects in metal by using infrared thermography," *International Journal of Applied Engineering Research*, Vol. 9, No. 24, pp. 29939-29948 (2014)
- [14] S. Ranjit, K. Kang, and W. Kim, "Investigation of lock-in infrared thermography for evaluation of subsurface defects size and depth," *International Journal of Precision Engineering and Manufacturing*, Vol. 16, No. 11, pp. 2255-2264 (2015)
- [15] S. Ranjit, M. Choi and W. Kim, "Quantification of defects depth in glass fiber reinforced plastic plate by infrared lock-in thermography," *Journal of Mechanical Science and Technology*, Vol. 30, No. 3, pp. 1111-1118 (2016)
- [16] R. Shrestha, J. Park and W. Kim, "Application of thermal wave imaging and phase shifting method for defect detection in stainless steel," *Infrared Physics & Technology*, Vol. 76, pp. 676-683 (2016)
- [17] R. C. Waugh, J. M. Dulieu-Barton and S. Quinn, "Defect detection using pulse phase thermography-repeatability and reliability of

- data," *Key Engineering Materials*, Vol. 569, pp. 1164-1169 (2013)
- [18] R. Waugh, J. Dulieu-Barton, and S. Quinn, "Modelling and evaluation of pulsed and pulse phase thermography through application of composite and metallic case studies," *NDT & E International*, Vol. 66, pp. 52-66 (2014)
- [19] C. Ibarra-Castanedo and X. Maldague, "Pulsed phase thermography reviewed," *Quantitative Infrared Thermography Journal*, Vol. 1, No. 1, pp. 47-70 (2004)
- [20] S. Pickering and D. Almond, "Matched excitation energy comparison of the pulse and lock-in thermography NDE techniques," *NDT & E International*, Vol. 41, No. 7, pp. 501-509 (2008)
- [21] X. Maldague and S. Marinetti, "Pulse phase infrared thermography," *Journal of Applied Physics*, Vol. 79, No. 5, pp. 2694-2698 (1996)
- [22] X. Maldague, S. Marinetti and J. Couturier, "Applications of pulse phase thermography," *Review of Progress in Quantitative Non-destructive Testing*, Vol 16, pp. 339-344 (1997)